Design of a Small NEMP Simulator for the Immunity Test of Core Electronic Components in HEMP Environments

YOUNG-JIN KIM[1], YOUNG-KYUNG JEONG[2], DONG-GI YOUN[2], (Member, IEEE),
HYUN HO PARK[3], (Senior Member, IEEE), AND YONG BAE PARK[4,5], (Senior Member, IEEE)

[1]Department of Military Digital Convergence, Ajou University, Gyeonggi-do 16499, South Korea
[2]Replex Company Ltd., Seoul 01811, South Korea
[3]Department of Electronic Engineering, The University of Suwon, Gyeonggi-do 18323, South Korea
[4]Department of Electrical and Computer Engineering, Ajou University, Gyeonggi-do 16499, South Korea
[5]Department of AI Convergence Network, Ajou University, Gyeonggi-do 16499, South Korea

Corresponding author: Yong Bae Park (yong@ajou.ac.kr)

ABSTRACT We design a small nuclear electromagnetic pulse (NEMP) simulator to study the immunity of core electronic components in high-altitude electro-magnetic pulse (HEMP) environments. The NEMP simulator comprises of a power device, a high-voltage charging part, a pulse-shaping part, and the input taper. The performance of the proposed simulator is verified by the actual experimental results. The positive and negative polarities for the mono pulse output of a transient pulse generator are checked against the standard. The field uniformity of the proposed NEMP simulator is 1.6 dB and fully meets the standard.

INDEX TERMS Nuclear electromagnetic pulse, high-altitude electromagnetic pulse, guided-wave electromagnetic pulse simulator, field uniformity.

I. INTRODUCTION

High-altitude electro-magnetic pulse (HEMP) is the electromagnetic (EM) pulse that is observed due to nuclear explosions at an altitude of 30 km and above [1], [2]. The IEC 61000-2-9 standard [1] established by the International Electronical Commission (IEC) categorizes the radiant environments of HEMP according to the creation of time. Furthermore, the mechanism of nuclear explosion at high altitudes was characterized by the peak electric fields of E1(early time), E2(intermediate time), and E3(late time), as well as fast rise time (10–90%) and pulse duration. HEMP has a peak electric field of 50–65 kV/m, a rise time of 0.9–4.6 ns, and a pulse width of 23–184 ns, covering a large area [2].

Previous studies on HEMP can be divided into two main categories. The first involves the HEMP generation process and the E1 signal. These studies were performed by simulating the explosions of nuclear weapons at high altitudes and converting gamma rays into EM energy via Compton

The associate editor coordinating the review of this manuscript and approving it for publication was Su Yan.

scattering, resulting in the formation of a HEMP on the surface of the environment [3]–[5]. Additionally, in the HEMP environment, the E1 signal exhibits the largest electric field intensity and a fast exponential waveform in nanoseconds. Therefore, HEMP has a large impact on electronic equipment, which has been studied extensively [4], [6]–[8].

The second is on NEMP simulators for artificially generated HEMP signals. These simulators have become an important mean of solving many problems that arise in the HEMP environments [9]. The implementation technique and standard of the E1 pulse characteristics of the NEMP simulator were summarized [6] and NEMP simulators were clearly explained in terms of their characteristics [10]. The NEMP simulator artificially generates the HEMP E1 pulse waveform for the HEMP process described above, to test the immunity of the equipment under test (EUT) for the HEMP E1 pulse [11].

According to the IEC standard [12] and Baum [13], the NEMP simulators are classified into three forms. These are 1) guided wave, 2) hybrid, and 3) dipole (radiating). The characteristics and experimental methods for each type have

IEEE *Access*

Y.-J. Kim *et al.*: Design of a Small NEMP Simulator for the Immunity Test of Core Electronic Components in HEMP Environments

been detailed in a previous study [7]. Several researchers have modeled HEMP signals according to the type of simulator and have achieved outcomes through all the three forms (guided wave [14]–[17], hybrid [18], [19], dipole [20]) by using only computer simulations. Also, the guided-wave simulator has four types of waveforms parallel, triangular, conical, and rhombi-plate [21].

In [22], fifteen measurement points in the guided-wave large NEMP simulator was undertaken using the Finite Integration Technique (FIT). The results of field uniformity were also analyzed by computational methods and real measurements.

In [23], the guided-wave of the parallel plate type was simulated on CST to find the optimal feed angle, which was found to be 18°. The prototype was modified with a hybrid parallel-plate/conical TEM-Line to meet MIL-STD-461G.

The previous NEMP simulators were generally large since the size of the EUT was larger than 1 m [15], [23]. Most of the recent electronic components are miniaturized and integrated. The small NEMP simulator has the advantage that only the core parts of the EUT can be disassembled and used for experiments in a test bed environment. It can be implemented in the laboratory and can be used for EMP coupling studies on small electronic components without setting up a larger NEMP simulator [24]. Also, the previous NEMP simulators have evaluated the immunity of the EUT at the system level, not the component level. However, it is becoming increasingly important to evaluate the immunity of the core components at the component level. Therefore, small NEMP simulators are required.

In [25], the small NEMP simulator has been proposed to simulate the transmission line circuit model using the time-domain reflections (TDR) method and predict the field strength. The results showed an error of less than 10% below 70 kV/m. Also, previous studies [22]–[23], [25] of NEMP simulator did not contain negative polarity for the mono pulse output of a transient pulse generator that was required by the specification [26].

In this paper, a small NEMP simulator is proposed. According to the equipment conditions of the MIL-STD-461G standard, the NEMP simulator requires both positive and negative polarities. It is necessary for electromagnetic compatibility (EMC) testing to enable negative polarity, and additional designs have been made to implement it. The step-by-step design process for the implementation of negative polarity is proposed by using a high voltage DC-DC negative converter within the high voltage charging part. In addition, the electric field strength experiment was conducted from low electric field strength to high electric field strength by combining spark gap and solenoid in the pulse shaping part. Capacitances of the high-voltage charging part and the field uniformity are calculated and the impedance considering the pulse waveform is predicted by using the computer simulation (MWS of CST). The performance of the NEMP simulator is verified by the experiments.

II. DESIGN OF NEMP SIMULATOR
A. DESIGN OVERVIEW
The EMP simulator has three types of guided-wave simulator, as shown in Fig. 1 [21]. In the parallel-plate simulator (PPS) method, the input taper (transmission line) is connected to the pulse generator, and it transmits a signal to induce the field with a working volume. This consists of three parts, which are 1) input taper, 2) parallel plate to the bottom surface, and 3) output taper. The PPS type simulator is advantageous in that the reflected wave and the field distortion are small. However, the length of the input taper is relatively long to obtain good characteristics for PPS. Additionally, the triangular-plate simulator (TPS) removes the horizontal parallel-plate section in the PPS form. The input taper is directly connected to the output taper in the middle of the simulator. This causes a drawback in that the reflected wave becomes larger in the middle region.
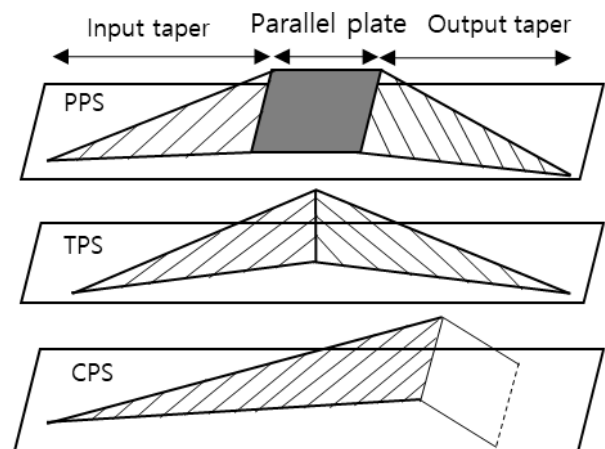

FIGURE 1. Guided-wave EMP simulator of categorization.

In the conical-plate simulator (CPS), the output taper is removed from the TPS form, as shown in Fig 2. Since the CPS uses only the input taper area as the working volume, it is suitable for testing a small electronic component. Inside the input taper, an electric field waveform similar to an electromagnetic wave in free space should be applied to the test object. This means that the pulse incident on the test object should be a transverse electromagnetic (TEM) wave with planar wave, as in free-space propagation [14], [27]. Therefore, the input taper is designed to reduce S11 (return
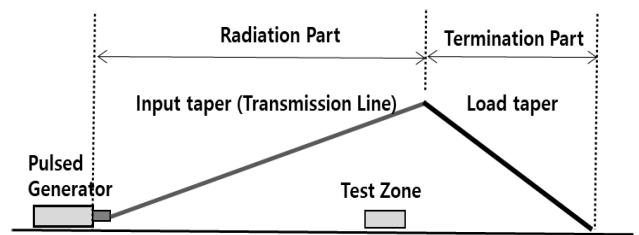

FIGURE 2. Side view of conical-plate simulator (CPS).

Y.-J. Kim *et al.*: Design of a Small NEMP Simulator for the Immunity Test of Core Electronic Components in HEMP Environments

IEEE*Access*

loss). In other words, it should be designed to reduce the reflected wave caused by the change in the characteristic impedance that occurs at the matching part of the input taper and termination part(impedance). Also, the TEM wave propagation in an electric field inside the working volume of the CPS-type NEMP simulator is expressed as (1) [15].

$$E = \frac{V}{h} \tag{1}$$

where E is the electric field strength in V/m, V is the voltage at the input port of the CPS in V, and h is the septum height in m. Therefore, in the overall design, the input voltage and height of the input taper must be considered. The design flow chart of NEMP simulator is shown in Fig. 3. For testing small core electronic component, the required maximum height is 500 mm. Consequently, the maximum input voltage of the pulse-shaping part must be 25 kV. The small NEMP simulator comprises a power device, a high-voltage charging section, a pulse-shaping part, and the input taper, as shown in Fig. 4.
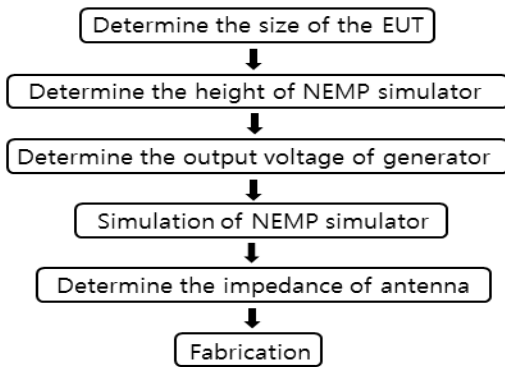

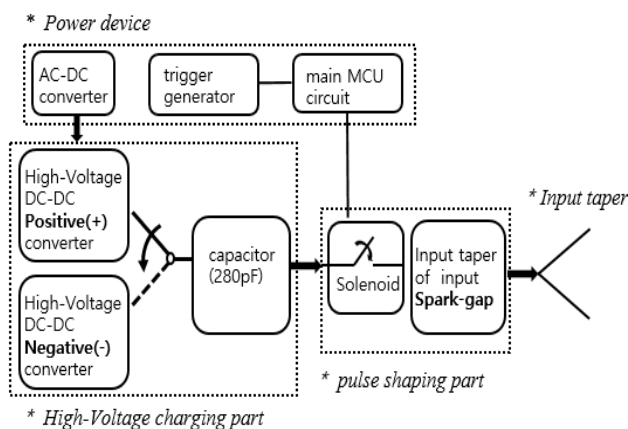**FIGURE 3.** Design flow chart of NEMP simulator.

FIGURE 4. Structural diagram of small NEMP simulator.

B. POWER DEVICE
The power device consists of an AC–DC converter that converts commercial AC power into DC power and a main micro controller unit (MCU) circuit that generates the control signal, and supplies power and the control signal to the

high-voltage charging part and pulse-shaping part. Power device transmit the high voltage DC–DC converter-driving waveform (8 V, 30 ms).

C. HIGH-VOLTAGE CHARGING PART
The high-voltage charging part uses a high-voltage DC–DC converter signal to charge the capacitor, by boosting a high voltage of several tens of kV with the power applied by the power device. In this part, positive and negative polarities are created and delivered to the capacitor by switch.

D. PULSE-SHAPING PART
The pulse-shaping part converts a charged voltage of 25 kV DC in the capacitor of the high-voltage charging part into a pulse through a solenoid and transmits it to the input taper. The solenoid then receives the control signal to operate from the main MCU circuit of the power device. In the solenoid operation, the 25-kV signal source is short-circuited using a spark gap. Through this, the signal source is transmitted to the input taper of the input unit ($\pm$ 25 kV, 30 ms), as shown in Fig 5.
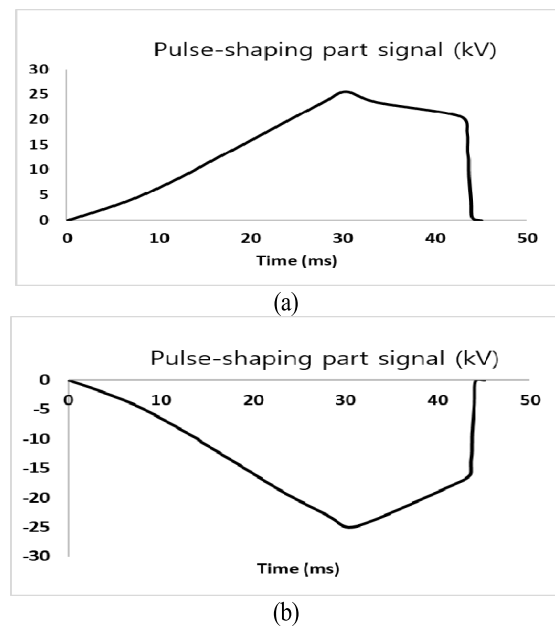

FIGURE 5. Measured output voltage of pulse-shaping part. (a) Positive. (b) Negative.

In the case of computer simulation of the pulse-shaping part, the excitation signal (25 kV, 2.54 ns) of the source stage applied to the discrete port, only the expected transient time is applied when the source switch is short-circuited. The excitation signal is shown in Fig. 6. Moreover, the source capacitance (SC) must be designed according to an arbitrary load resistor value. The SC of the simulation is from the capacitor physically mounted inside the discrete port source; assuming a load resistance of 100 Ω. This means that this value is selected to satisfy the full width at half maximum (FWHM) during the normal RC discharge. When R = 100 Ω

IEEE *Access*

Y.-J. Kim *et al.*: Design of a Small NEMP Simulator for the Immunity Test of Core Electronic Components in HEMP Environments
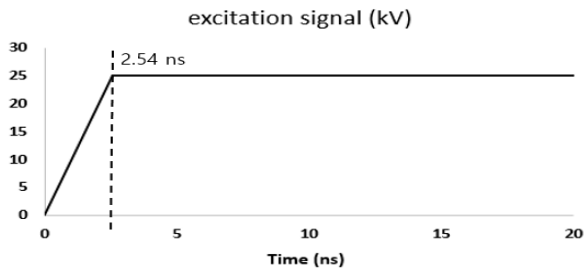
FIGURE 6. Excitation signal(simulation) applied to discrete port.

and $C = 280 \times 10^{-12}$ F in the RC discharge (2) assuming that the switch short-circuit transient time is t, the current I flowing through the input taper becomes 50% of the maximum value is approximately 19.4 ns, which satisfies FWHM.

$$I = \frac{V_o}{R} e^{-t/RC} \tag{2}$$

E. SIMULATION OF THE INPUT TAPER AND IMPEDANCE

Electric field of a HEMP E1 pulse is generated inside the input taper using the excitation signal applied in the pulse-shaping part. In general, the input taper of a large NEMP simulator required to meet MIL-STD-461G uses a metal wire. This is because it is difficult to reduce the EMP rising time using metal plates due to the occurrence of corona and high impedance [22], [28]. However, small NEMP simulators can be designed using metal plates as they are less impacted by above problems. As presented in Fig. 7, the input taper part was designed in the form of a metal plate and design parameter with simulation is shown on table 1.

TABLE 1. Design parameter with simulation.

No.	Design Parameters	Computed value
1	input taper length	1,290 mm
2	input taper plate width	690 mm
3	height	500 mm
4	bottom plate	2,160 * 1,090 mm
5	conic angle	25.49 °
6	impedance	100 Ω
7	excitation signal (peak pulse voltage)	25 kV
8	metal plate	Perfect Electric Conductor (PEC)

Impedance matching is important for the input taper because it changes the waveform shape. A poor matching between input taper and termination part(impedance) can destroy the target pulse waveforms even if the other parts of the simulator have been designed well [14]. For parallel plates, the impedance can be calculated by using the transmission line equation [29], [30]. In the TEM horn antennas, the impedance can be calculated by considering the width and height of the input taper [31], [32]. In the case of small-NEMP simulators in the type of CPS, a formalized waveform
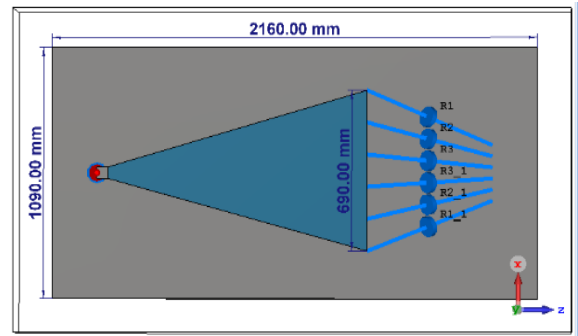
(a)
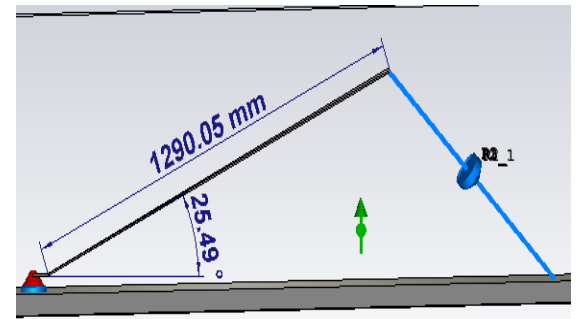
(b)

FIGURE 7. The simulation model of small NEMP simulator. (a) Top view (b) Side view.

(a peak amplitude of 50 kV/m, an FWHM of 23 ± 5 ns, and a rise time (peak amplitude of 10 % to 90 %) of 1.8–2.8 ns) is required [26]. So, it is necessary to calculate the impedance considering the waveform by using computer simulation (MWS of CST). Fig. 8 and Table 2 show the waveform in terms of the impedances from 50 Ω to 377 Ω. At the intrinsic impedance (377 Ω), the largest field strength was 71 kV/m; however, the formalized waveform was obtained
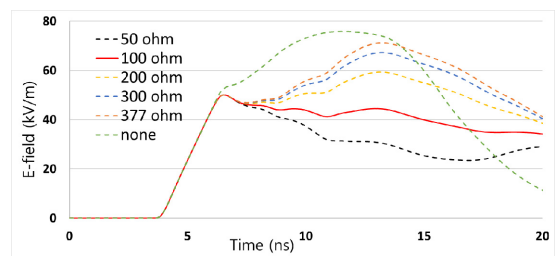
FIGURE 8. Electric field waveforms with varying impedance.

TABLE 2. Simulation results.

Impedance	Peak	FWHM	Rise	Result
	50 kV/m	23 ± 5 ns	1.8–2.8 ns	Pass/Fail
50	49.96	9.14	2.66	Fail
100	52,10	21.07	2.58	Pass
200	59.31	19.32	8.92	
300	67.16	15.87	9.03	Fail
377	71.88	14.89	9.27	
none	75.79	11.42	7.69	

Y.-J. Kim *et al.*: Design of a Small NEMP Simulator for the Immunity Test of Core Electronic Components in HEMP Environments

IEEE *Access*

when the impedance was 100 Ω. Normally, the NEMP simulator is terminated by a characteristic impedance, typically in the range of 80–100 Ω, at the end of the line [33]. In the above method, a load resistance of 600 Ω was used for all six parallel lines, and the total resistance value was set to 100 Ω. The components of the electric field are E_x, E_y, and E_z. The difference between E_y and other components is greater than 7dB since the direction of the E-field probe is the Y-axis.

III. MEASUREMENT

All designs were completed using computer simulation, and the fabricated prototype is shown in Fig. 9.
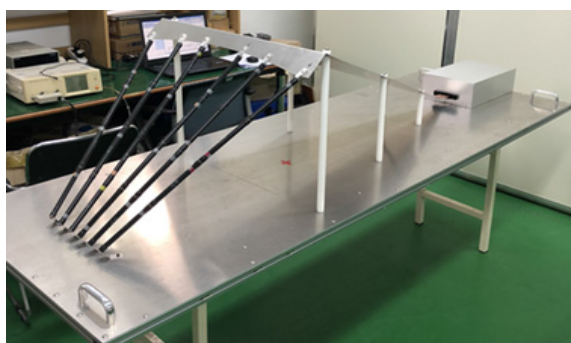

FIGURE 9. Fabrication of small NEMP simulator.

A. EXPERIMENT OF ELECTRIC FIELD STRENGTH

As presented in Fig. 10, the experiment of electric field strength was performed in an anechoic chamber for accurate measurements. A D-dot probe (Montena SFE35G) and a digital oscilloscope were used to measure the waveforms. The measurement position of a D-dot probe was 50mm from the bottom of metal plate. The measurement result was compared with the simulation results, which are shown in Fig. 11 and Table 3. Despite a pulse delay time of 4.27 ns between the measurement and the simulation, the measured peak, FWHM, and rise time were consistent with the simulation results.
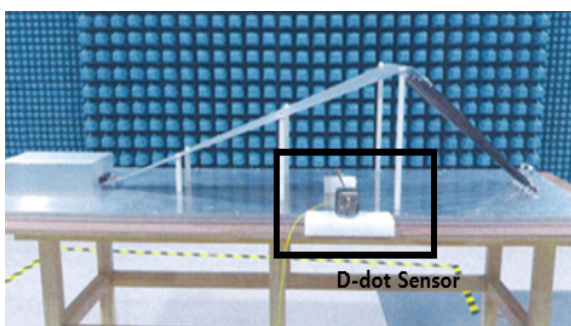

FIGURE 10. Measurements in an anechoic chamber.

Measurement is conducted according to the standard method. It was necessary to increase the pulse amplitude in two steps until the required 50 kV/m was reached. Also, the negative polarity was thoroughly examined since the standard requires both positive and negative polarities for the
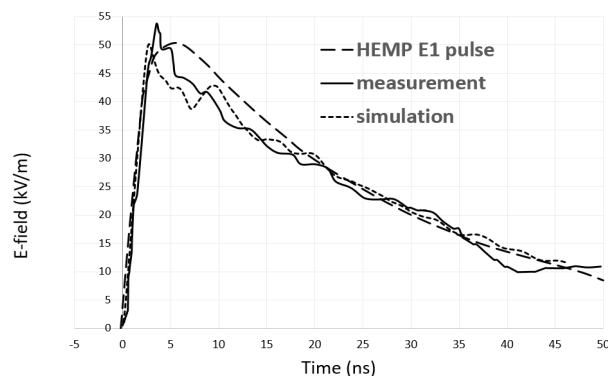

FIGURE 11. Measurement result compared with simulation.

TABLE 3. Measurement compared with simulation.

Contents	Peak(kV/m)	FWHM (ns)	Rise(ns)
HEMP E1 pulse	50.00	23 ± 5	1.8–2.8
measurement	54.14	21.68	2.22
simulation	50.83	21.07	2.04

mono pulse output of the transient pulse generator. Negative polarity must be activated on the electromagnetic compatibility (EMC) test, as both polarities were required in the electromagnetic immunity experiment [34]. The measurement results of the pulse amplitude are shown in Table 4 and Table 5 for positive polarity and negative polarity, respectively. The targeted pulse amplitude is very similar to the measurement. The main purpose of the military electronic equipment immunity test of MIL-STD-461G and the general electronic equipment immunity test of IEC 61000 is performed to determine a

TABLE 4. Pulse amplitude of positive polarity.

Pulse amplitude	Peak	FWHM	Rise
	50 kV/m	23 ± 5 ns	1.8–2.8 ns
5kV/m (10%)	6.06	22.77	2.33
10kV/m (20%)	12.69	20.88	2.60
20kV/m (40%)	22.34	21.22	2.44
40 kV/m (80%)	44.46	20.01	2.23
50kV/m (100%)	54.14	21.68	2.22

TABLE 5. Pulse amplitude of negative polarity.

Pulse amplitude	Peak	FWHM	Rise
	50 kV/m	23 ± 5 ns	1.8–2.8 ns
-5kV/m (10%)	(-) 6.12	19.88	2.33
-10kV/m (20%)	(-) 12.60	19.13	2.22
-20kV/m (40%)	(-) 23.22	20.33	2.33
-40 kV/m (80%)	(-) 42.24	20.44	2.33
-50kV/m (100%)	(-) 49.06	21.40	2.22

weak immunity level of the electronic equipment. Therefore, measurements are made by varying the electric field strength to several levels from the lowest strength (10 %) to the highest strength (100 %).

B. EXPERIMENT OF FIELD UNIFORMITY

The field uniformity is crucial to ensure the validity of results of the EUT in the electromagnetic field [34]. It is important that the proper field uniformity is formed inside the small NEMP simulator's input taper. According to MIL-STD-461G, five measuring points must be set inside the input taper, the uncertainty on the peak value of the electric field is 0 dB $\leq$ magnitude $\leq$ 6 dB, and the rise time and FWHM values must also be met [26]. The field uniformity is given by (3), (4), (5) [35], [36].

$$field\ uniformity = 20\log\frac{E + 1.15 \cdot s}{E - 1.15 \cdot s} \qquad (3)$$

where E is the mean value and s is the standard deviation as

$$E = \frac{1}{n}\sum_{i=1}^{n} E_i \qquad (4)$$

$$s = \sqrt{\frac{1}{n-1}\sum_{i=1}^{n}(E_i - E)^2} \qquad (5)$$

The MIL-STD-461G requires five measurement positions for the field uniformity, but the additional measurements were made for nine measurement positions. Fig. 12 shows the measurement position (0.2 m length $\times$ 0.2 m width) of each point in the field uniformity of the small NEMP simulator and the measurement results are listed in Table 6. The results of the measurement are 1.6 dB and 1.3 dB for five and nine
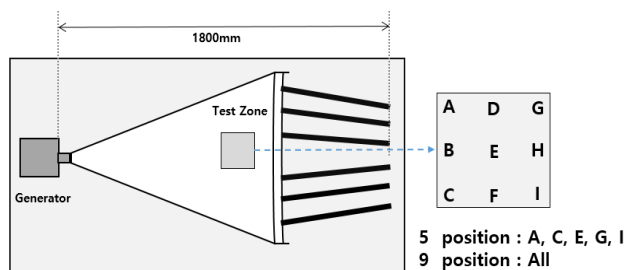
measurement positions. These results meet the MIL-STD-461G standard for the field uniformity. Note that there is only a slight difference in the field uniformity even if the measurement position of each point is shifted a little bit. Large NEMP simulators do not have a directionality due to the isotropic radiation pattern [37]. For large NEMP simulators, the field uniformities (1.0 m length $\times$ 1.0 m width) are is 3.6 dB and 3.5 dB for five and nine measurement positions, respectively [22]. Thus, the field uniformity of the proposed small NEMP simulator is 2 dB better at five measurement positions and 2.2 dB better at nine measurement positions than the large NEMP simulator. This improvement of the field uniformity is the result of using both the spark-gap and the solenoid in the pulse shaping part. If the output voltage of pulse-shaping part is less than 10 kV, a solid-state switch can be used to generate an accurate output voltage. The accurate output voltage can reduce the deviation of the electric field strength and achieve the good results of field uniformity. However, the maximum output voltage of the pulse-shaping part of our simulator is 25 kV according to equation (1). Therefore, a non-solid state switch, i.e. spark gap should be used instead of the solid-state switch [38] and the output voltage inevitably deviates due to the characteristics of the spark gap. To solve this problem, the pulse-shaping part was implemented with a spark-gap and a solenoid. Fig. 13 shows a fabricated the pulse-shaping part. The solenoid makes the spark gap into a short circuit when it receives an electrical control signal. Then DC 25 kV charged in the capacitor of the high-voltage charging part is applied to the input taper through the spark gap. The solenoid can compensate the output voltage deviation of the spark gap. The solenoid uses a triggered method and it triggers immediately when the targeted voltage is charged in the spark gap, thus the spark gap has a smaller voltage deviation than the self-triggered method. In addition, it always makes a constant peak pulse voltage as shown in Fig. 14. A constant peak pulse voltage is applied to the input taper through the

FIGURE 12. Positions of each point in field uniformity.

TABLE 6. According to position of measurement (9 position).

Position	Peak	FWHM	Rise
	50 kV/m	23 ± 5 ns	1.8–2.8 ns
A	59.24	22.79	2.85
B	57.17	23.15	2.33
C	58.77	21.78	2.23
D	57.33	22.49	2.35
E	55.37	24.17	2.37
F	53.22	23.88	2.42
G	49.50	21.22	2.41
H	52.13	24.16	2.34
I	51.66	22.45	2.12
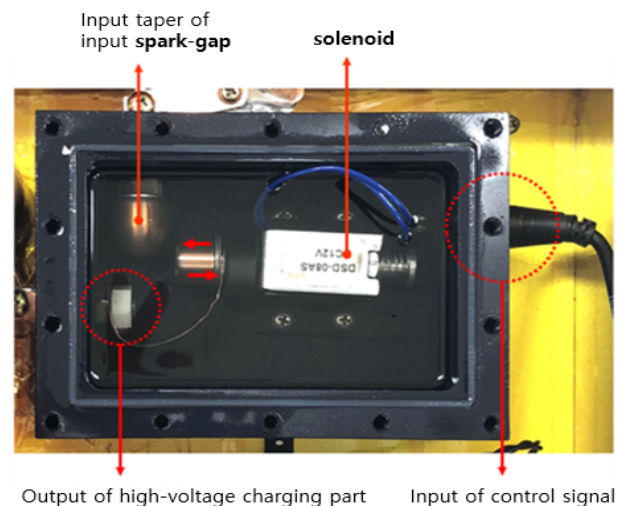
FIGURE 13. Spark-gap and solenoid in the pulse-shaping part.

Y.-J. Kim *et al.*: Design of a Small NEMP Simulator for the Immunity Test of Core Electronic Components in HEMP Environments
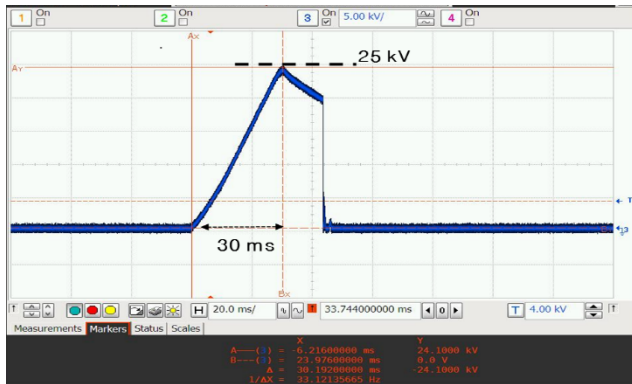
IEEE *Access*

FIGURE 14. Output voltage of spark-gap in the pulse-shaping part.

spark gap, and the electric field is formed uniformly inside the input taper. Another reason to use a solenoid is to get low voltage to high voltage to create an electric field from 5 kV/m to 50 kV/m. Therefore, it is possible because the targeted voltage is charged in the spark-gap and accurate output can be performed using a solenoid. (ex. output voltage of spark-gap: 2.5 kV, electric field: 5 kV/m (10 %) ∼ output voltage of spark-gap: 25 kV, 50 kV/m (100 %)). As a result, we obtained the improved results of the accuracy for the electric field strength and field uniformity by combining the spark-gap and the solenoid. The proposed NEMP simulator has the advantage of obtaining accurate results for the component level measurements.

IV. CONCLUSION

A small NEMP simulator was proposed to investigate the immunity of small electronic component in HEMP environments. The measured field strength was 54.1 kV/m, the FWHM was 21.6 ns, and the rise time was 2.2 ns, which were within an error of 5% of the simulation results. Also, the measured result satisfies the positive and negative polarities of the transient pulse generator mono pulse output, as specified in the equipment conditions. The field uniformity of the small simulator is 1.6 dB and fully meets the standard. To design the negative polarity, a high voltage DC-DC negative converter was used in the high voltage charging part and it was possible by combining the spark gap and solenoid in the pulse shaping part to design the desired electric field strength. Our small NEMP simulator can make accurate electric field strength for good field uniformity.

REFERENCES

[1] *Electromagnetic Compatibility (EMC)-Part 2: Environment-Section 9: Description of HEMP Environment-Radiated Disturbance*, Standard IEC 61000-2-9 Ed. 1.0, 1996-2002, 1996. [Online]. Available: https://www.iec.ch

[2] R. Hoad and W. A. Radasky, "Progress in high-altitude electromagnetic pulse (HEMP) standardization," *IEEE Trans. Electromagn. Compat.*, vol. 55, no. 3, pp. 532–538, Jun. 2013.

[3] C. Meng, "Numerical simulation of the HEMP environment," *IEEE Trans. Electromagn. Compat.*, vol. 55, no. 3, pp. 440–445, Jun. 2013.

[4] C. D. Eng, "Development of the time dependence of the nuclear (E1) HEMP electric field," *IEEE Trans. Electromagn. Compat.*, vol. 53, no. 3, pp. 737–748, Aug. 2011.

[5] W. A. Farmer and A. Friedman, "Effect of multiple scattering on the Compton recoil current generated in an EMP, revisited," *IEEE Trans. Nucl. Sci.*, vol. 62, no. 4, pp. 1695–1706, Aug. 2015.

[6] D. V. Giri and W. D. Prather, "High-altitude electromagnetic pulse (HEMP) risetime evolution of technology and standards exclusively for E1 environment," *IEEE Trans. Electromagn. Compat.*, vol. 55, no. 3, pp. 484–491, Jun. 2013.

[7] A. Wraight, W. D. Prather, and F. Sabath, "Developments in early-time (E1) high-altitude electromagnetic pulse (HEMP) test methods," *IEEE Trans. Electromagn. Compat.*, vol. 55, no. 3, pp. 492–499, Jun. 2013.

[8] H. Xie, Y. Li, and J. Wang, "Empirical formula of effective coupling length for transmission lines illuminated by E1 HEMP," *IEEE Trans. Electromagn. Compat.*, vol. 58, no. 2, pp. 581–587, Apr. 2016.

[9] D. V. Giri and F. M. Tesche, "Classification of intentional electromagnetic environments (IEME)," *IEEE Trans. Electromagn. Compat.*, vol. 46, no. 3, pp. 322–328, Aug. 2004.

[10] J. C. Giles and W. D. Prather, "Worldwide high-altitude nuclear electromagnetic pulse simulators," *IEEE Trans. Electromagn. Compat.*, vol. 55, no. 3, pp. 475–483, Jun. 2013.

[11] N. S. Manisha, "Design of bounded wave NEMP (RS105) test simulator," in *Proc. 15th Int. Conf. Electromagn. Interference Compat. (INCEMIC)*, Nov. 2018, pp. 1–4.

[12] *Electromagnetic Compatibility (EMC): Part 4. Testing and Measurement Techniques-Section 32: HEMP Simulator Compendium*, Standard IEC 61000-4-32, 2002. [Online]. Available: https://www.iec.ch

[13] C. Baum, "EMP simulators for various types of nuclear EMP environments: An interim categorization," *IEEE Trans. Electromagn. Compat.*, vol. EMC-20, no. 1, pp. 35–53, Feb. 1978.

[14] C. Wang, D. Xie, N. Wu, and W. Song, "On the pulsed fields waveform dependent characteristics of NEMP simulation," in *Proc. Int. Conf. Electromagn. Adv. Appl.*, Sydney, NSW, Australia, Sep. 2010, pp. 770–773.

[15] J. Cai, B. Wang, F. Hu, D. Zeng, and G. Guo, "The design and property analysis of small wave bounded EMP simulator," in *Proc. Int. Conf. Comput., Mechatronics, Control Electron. Eng.*, Changchun, China, Aug. 2010, pp. 456–459.

[16] G. Haiguang, W. Guanghui, and P. Xiaodong, "Time-domain simulation research on EMP simulator with fast rise-time," in *Proc. 8th Int. Conf. Electron. Meas. Instrum.*, Aug. 2007, pp. 1–161.

[17] J. J. A. Klaasen, "An efficient method for the performance analysis of bounded-wave nuclear EMP simulators," *IEEE Trans. Electromagn. Compat.*, vol. 35, no. 3, pp. 329–338, Aug. 1993.

[18] R. Kichouliya and M. J. Thomas, "Design of a hybrid nuclear electromagnetic pulse simulator," in *Proc. 13th Int. Conf. Electromagn. Interference Compat. (INCEMIC)*, Visakhapatnam, India, Jul. 2015, pp. 92–97.

[19] Y. Wang, Y. Chen, and L. Fan, "Simulation for several kinds of TEM horn antenna used by NEMP simulator," in *Proc. Int. Appl. Comput. Electromagn. Soc. Symp. (ACES)*, Suzhou, China, Aug. 2017, pp. 1–3.

[20] S.-Q. Zheng and F. Deng, "Two types of antenna optimizing design for EMP simulator," in *Proc. IEEE 6th Int. Symp. Microw., Antenna, Propag., EMC Technol. (MAPE)*, Shanghai, China, Oct. 2015, pp. 86–90.

[21] P. A. A. Scvat, "Design of a bounded wave EMP simulator (intended as second stage simulator for DREO)," Defence Res. Establishment, Ottawa, ON, Canada, Tech. Rep. 1008, Jun. 1989.

[22] L. Yao, T. Shen, N. Kang, D. Liu, and J. Huang, "Time-domain simulation and measurement of a guided-wave EMP Simulator's field uniformity," *IEEE Trans. Electromagn. Compat.*, vol. 55, no. 6, pp. 1187–1194, Dec. 2013.

[23] M. B. Lara, J. R. Mayes, C. Nunnally, W. C. Nunnally, J. M. Byman, and D. Kohlenberg, "Computer-controlled RS-105 test system for 1-M EUTS," in *Proc. IEEE Pulsed Power Conf. (PPC)*, Austin, TX, USA, May 2015, pp. 1–4.

[24] R. Kichouliya and M. J. Thomas, "Experimental simulation of low level hybrid electromagnetic pulse (EMP) for vulnerable studies on electronic sytems and cables," in *Proc. Int. Conf. Microelectron., Comput. Commun. (MicroCom)*, Jan. 2016, pp. 1–6.

[25] S. Ranade, G. Verma, and G. Shende, "TDR analysis of the conical plate NEMP simulator using a proposed transmission line circuit model," in *Proc. 13th Int. Conf. Electromagn. Interference Compat. (INCEMIC)*, Visakhapatnam, India, Jul. 2015, pp. 32–35.

[26] *Requirements for the Control of Electromagnetic Interference Emissions and Susceptibility*, Standard MIL-STD-461G, Dec. 2015.

[27] R. W. P. King, D. J. Blejer, and T. T. Wu, "Standing waves and notches in an EMP simulator and their reduction," *IEEE Trans. Electromagn. Compat.*, vol. EMC-23, no. 2, pp. 80–87, May 1981.

IEEE *Access*

Y.-J. Kim *et al.*: Design of a Small NEMP Simulator for the Immunity Test of Core Electronic Components in HEMP Environments

[28] X. Pan, G. Wei, and X. Ren, "Electromagnetic characteristic influence caused by metal wire grating replacing metal board in bounded-wave simulator," *J. Ordnance Eng. Coll.*, vol. 18, pp. 29–32, Sep. 2006.

[29] R. Ma, L. Shi, Y. Zhou, and X. Zhang, "Comparison of the bounded-wave simulator with ellipse-arc transition and tapered transition," in *Proc. 6th Asia–Pacific Conf. Environ. Electromagn. (CEEM)*, Nov. 2012, pp. 238–241.

[30] X. Xu, J. Luo, X. Lee, Z. Yao, and C. Yu, "A high-repetition-rate bounded-wave EMP simulator based on hydrogen thyratron and transmission line transformer," *IEEE Trans. Plasma Sci.*, vol. 40, no. 12, pp. 3499–3507, Dec. 2012.

[31] A. Zhang, L. Wang, C. Guo, and Y. Jiang, "Constant impedance TEM horn antenna: Aperture and characteristic impedance's impacts on axial electric field," *J. Infr., Millim., Terahertz Waves*, vol. 30, no. 10, pp. 1067–1072, Jun. 2009.

[32] H. Choi and S. Lee, "Design of an exponentially-tapered TEM horn antenna for the wide broadband communication," *Microw. Opt. Technol. Lett.*, vol. 40, no. 6, pp. 531–534, Mar. 2004.

[33] D. V. Giri, "Design guidelines for flat-plate conical guided-wave EMP simulators with distributed terminators," *Sensor Simul. Note*, vol. 402, pp. 1–37, Oct. 1996.

[34] *Electromagnetic Compatibility (EMC)—Part 4-3: Testing and Measurement Techniques—Radiated, Radio-Frequency, Electromagnetic Field Immunity Test*, Standard IEC 6l000-4-3:2020, 2020. [Online]. Available: https://www.iec.ch

[35] *Electromagnetic Compatibility (EMC)—Part 4-20: Testing and Measurement Techniques—Emission and Immunity Testing in Transverse Electromagnetic (TEM) Waveguides*, Standard IEC61000-4-20:2010, 2010. [Online]. Available: https://www.iec.ch

[36] C. Groh, J. P. Karst, M. Koch, and H. Garbe, "TEM waveguides for EMC measurements," *IEEE Trans. Electromagn. Compat.*, vol. 41, no. 4, pp. 440–445, Nov. 1999.

[37] Y.-G. Chen, Y. Wang, and Q.-G. Wang, "A new type of TEM horn antenna for high-altitude electromagnetic pulse simulator," *IEEE Antennas Wireless Propag. Lett.*, vol. 12, pp. 1021–1024, 2013.

[38] P. C. Saroj, M. R. Kulkarni, S. Kumar, V. Sharma, S. Mitra, P. Patade, A. Sharma, and K. C. Mittal, "Synchronization and reliable operation of triggered spark gap switches in 40 kJ, 20 kV EMM system," in *Proc. Int. Symp. Discharges Electr. Insul. Vac. (ISDEIV)*, Sep. 2014, pp. 353–355.

YOUNG-KYUNG JEONG received the M.S. degree in computer science and engineering from Changwon University, Changwon, South Korea, in 1999, and the Ph.D. degree with the Department of Electrical and Computer Engineering, University of Seoul, Seoul, South Korea, in 2015. He is currently a Researcher-in-Charge with Replex Company Ltd., Seoul. His research interests include the HPEM and pulsed power systems.

DONG-GI YOUN (Member, IEEE) received the M.S. and Ph.D. degrees in electronics engineering from Kyungnam University, Changwon, South Korea, in 1997 and 2000, respectively. He is currently a Chief Executive Officer with the Replex Company Ltd., Seoul, South Korea. His research interests include the HPEM and RF engineering.

HYUN HO PARK (Senior Member, IEEE) received the Ph.D. degree in electrical engineering from the Korea Advanced Institute of Science and Technology, Daejeon, South Korea, in 1999.
He is currently an Assistant Professor with The University of Suwon, Hwaseong, South Korea. His research interests include computational electromagnetics, system-level electromagnetic interference (EMI) design, signal/power integrity in high-speed digital system design, and integrated circuit/module-level EMI evaluation and measurement techniques.

YOUNG-JIN KIM received the B.S. degree in electronics engineering from Korea University, South Korea, in 2011, and the M.S. degree in electronic engineering from Ajou University, South Korea, in 2014, where he is currently pursuing the Ph.D. degree with the Department of Military Digital Convergence. He also works with the Korea Testing and Research Institute (KTR), Gwacheon, South Korea, as a Head Researcher. His current research interests include electromagnetic compatibility and high-power electromagnetic pulse.

YONG BAE PARK (Senior Member, IEEE) received the B.S., M.S., and Ph.D. degrees in electrical engineering from the Korea Advanced Institute of Science and Technology, South Korea, in 1998, 2000, and 2003, respectively. From 2003 to 2006, he was with the Korea Telecom Laboratory, Seoul, South Korea. In 2006, he joined the School of Electrical and Computer Engineering, Ajou University, South Korea, where he is currently a Professor. His research interests include electromagnetic field analysis, electromagnetic compatibility, and metamaterial antennas.

• • •